A numerical model for the transport of salinity in estuaries

F. Navarrina[1], I. Colominas[1,*,†], M. Casteleiro[1], L. Cueto-Felgueroso[2],
H. Gómez[3], J. Fe[1] and A. Soage[1]

[1]*GMNI—Grupo de Métodos Numéricos en Ingeniería, Department of Applied Mathematics, Universidad de A Coruña, E.T.S. de Ingenieros de Caminos, Canales y Puertos, Campus de Elviña, 15071 A Coruña, Spain*
[2]*Aerospace Computational Design Laboratory, Department of Aeronautics & Astronautics, Massachusetts Institute of Technology, 77 Massachusetts Avenue, Cambridge, MA 02139, U.S.A.*
[3]*The Institute for Computational Engineering and Sciences (ICES), University of Texas, 1 University Station, Austin, TX 78712, U.S.A.*

SUMMARY

In this paper, a numerical model for the simulation of the hydrodynamics and of the evolution of the salinity in shallow water estuaries is presented. This tool is intended to predict the possible effects of Civil Engineering public works and other human actions (dredging, building of docks, spillages, etc.) on the marine habitat, and to evaluate their environmental impact in areas with high productivity of fish and of seafood. The prediction of these effects is essential in the decision making about the different options that could be implemented.

The mathematical model consists of two coupled systems of differential equations: the shallow water hydrodynamic equations (that describe the evolution of the depth and of the velocity field) and the shallow water advective–diffusive transport equation (that describes the evolution of the salinity level).

Some important issues that must be taken into account are the effects of the tides (including that the seabed could be exposed), the volume of fresh water provided by the rivers and the effects of the winds. Thus, different types of boundary conditions are considered.

The numerical model proposed for solving this problem is a second-order Taylor–Galerkin finite element formulation.

The proposed approach is applied to a real case: the analysis of the possible effects of dredging *Los Lombos del Ulla*, a formation of sandbanks in the Arousa Estuary (Galicia, Spain).

A number of simulations have been carried out to compare the actual salinity level with the predicted situation if the different dredging options were executed. Some of the obtained results are presented and discussed. Copyright © 2007 John Wiley & Sons, Ltd.

*Correspondence to: I. Colominas, Civil Engineering School, Universidad de A Coruña, Campus de Elviña, 15071 A Coruña, Spain.
†E-mail: icolominas@udc.es

WILEY InterScience®
DISCOVER SOMETHING GREAT

1. BACKGROUND

Los Lombos del Ulla is a natural formation of sandbanks, lying downstream the Ulla River, within the tidal Arousa Estuary (*La Ría de Arousa*) in Galicia (northwestern region of SPAIN, EU). Figure 1 shows the whole estuary. The Ulla River and *Los Lombos del Ulla* are located in the upper right corner of the image. Figure 2 shows the geographical position of the estuary.

   The area is very rich in seafood, specially in bivalves: clams, cockles, mussels, scallops, etc. Hence, farming of bivalves is a major economic issue and the source of an extensive complementary industry (restaurants, fish canning factories, etc.).

Figure 1. Satellite image of the Arousa Estuary [Courtesy of VideaLAB, ETSICCP–UDC].
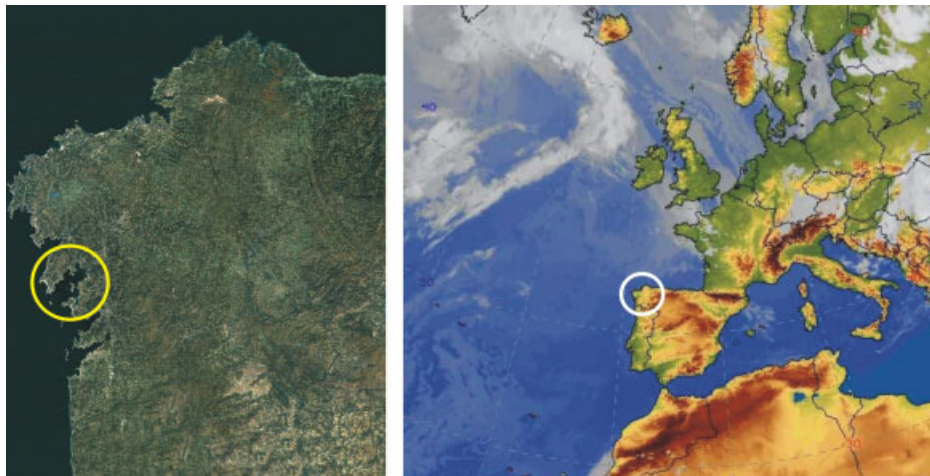

Figure 2. Satellite image of Galicia and stereographic polar image of Spain [Courtesy of VideaLAB, ETSICCP–UDC and of *Instituto Nacional de Meteorología*].

Figure 3. *Los Lombos del Ulla circa* 1995 [Courtesy of VideaLAB, ETSICCP–UDC].

Sand was regularly extracted from the Ulla River in the past. However, this practice is strictly forbidden by the environmental laws since a few decades. Thus, the ban on sand extraction could be speeding up the accumulation of sediments in the zone (see Figure 3).

The fishermen unions fear that the reducing depth due to the accumulation of sediments, with the concourse of the winds and of the high volume of fresh water provided by the river, could be slowing down the mixing, which could cause the drop of the salinity level in the zone due to the stagnation of fresh water.

Recent biological studies show that a slight fall in the salinity level is associated with an expected proportional fall in the shellfish productivity. And, if further falls in the salinity level occur, most individuals in the bivalve colonies could die, although entire colonies of some species would try to migrate in search for better living conditions (letting themselves to be dragged by the flow). Therefore, the gradual accumulation of sediments in *Los Lombos* could cause a permanently low level of salinity in the area, and the consequent huge loss in the local shellfish industry.

By the early 1990s, the Spanish coastal authorities considered several options in an attempt to restore the navigation conditions and to mitigate the supposedly harmful effects of the accumulation of sediments on the shellfish productivity. The proposed solution was the dredging of a channel in the direction of the main stream. However, the dredging was not entirely carried out, due to the environmental impact of some badly implemented operations and to the complaints of the affected fishermen.

In 2002, the *Xunta de Galicia* (the Regional Government) started to design a new plan for *Los Lombos del Ulla* with the following two goals: (a) to preserve the shellfish productivity; and (b) to restore the navigation conditions in the area. Two actions were initially considered: (1) to dredge a navigation channel (as it had been proposed about a decade before); and (2) to dredge the whole area, in order to increase the depth. In fact, the latter became an unyielding demand of the fishermen unions.

The main objective of this project was the development of a numerical model that could be used to evaluate the effect of the proposed actions on the shellfish productivity of the zone [1, 2].

Furthermore, the information provided by this tool would be used to assess the undesirable side effects of the possible actions (changes in the hydrodynamics of the zone), to evaluate the medium-term and the long-term stability of the sandbanks (the future possible accumulation of sand), and to evaluate the environmental impact of the works (the possible stirring and dragging of solid particles of the seabed and/or their diffusion to other areas).

2. MATHEMATICAL MODEL

In essence, two coupled models must be considered: a hydrodynamic model (to obtain the velocity field) and an advective–diffusive transport model (to predict the evolution of the salinity level).

Some important issues that must be taken into account are the effects of the tides (including that the seabed could be exposed) the volume of water provided by the Ulla River and the effects of the winds.

The Arousa Estuary can be considered a shallow water domain, since the depth is small when compared to the other two spatial dimensions. Therefore, the hydrodynamic phenomena can be adequately described by means of the shallow water hydrodynamic equations [3, 4].

This is a known 2D model that is obtained by vertical integration of the Navier–Stokes equations [5]. In essence, in this approach one assumes that the vertically averaged velocity at each point can be considered representative of the velocity field in the corresponding vertical column of water.

In a similar way, we expect the vertically averaged salinity at each point to be representative of the salinity field in the corresponding vertical column of water. Thus, the transport of salt can be adequately described by means of a shallow water-type transport model [3, 6–8] that is obtained by vertical integration of the advection–diffusion equations [5].

The registers of salinity in *Los Lombos* show that the vertical distribution is almost uniform, with a very weak stratification in the area of interest. Hence, it seems that there is no need to implement a multiple-layer model in this case.

Thus, for each point (x, y), at each time step t, the unknowns to be computed will be the depth $h(x, y, t) = z(x, y, t) - z_b(x, y)$, where $z(x, y, t)$ is the sea surface height and $z_b(x, y)$ is the seabed height, the velocity vector $\mathbf{v}(x, y, t) = [v_x(x, y, t), v_y(x, y, t)]^{\mathrm{T}}$ (vertical average of the horizontal velocity) and the salinity $c(x, y, t)$ (vertical average of the salt concentration).

Then, the whole set of shallow water equations (hydrodynamic and transport) can be written in a conservative form [3, 5] as

$$\frac{\partial \mathbf{u}}{\partial t} + \frac{\partial \mathbf{F}_x}{\partial x} + \frac{\partial \mathbf{F}_y}{\partial y} = \mathbf{R}^{\mathrm{S}} + \frac{\partial \mathbf{R}_x^{\mathrm{D}}}{\partial x} + \frac{\partial \mathbf{R}_y^{\mathrm{D}}}{\partial y}, \quad \mathbf{u} = \begin{Bmatrix} h \\ h v_x \\ h v_y \\ h c \end{Bmatrix} \tag{1}$$

being the so-called source term

$$\mathbf{R}^{\mathrm{S}} = \begin{Bmatrix} 0 \\ f h v_y + g(h - H)\dfrac{\partial}{\partial x}H + \tau_x \rho^{-1} - n^2 g h^{-1/3}|\mathbf{v}|v_x \\ -f h v_x + g(h - H)\dfrac{\partial}{\partial y}H + \tau_y \rho^{-1} - n^2 g h^{-1/3}|\mathbf{v}|v_y \\ 0 \end{Bmatrix} \tag{2}$$

being the so-called inviscid flux terms

$$\mathbf{F}_x = \left\{ \begin{array}{c} hv_x \\ hv_x^2 + \frac{1}{2}g(h^2 - H^2) \\ hv_x v_y \\ hcv_x \end{array} \right\}, \quad \mathbf{F}_y = \left\{ \begin{array}{c} hv_y \\ hv_x v_y \\ hv_y^2 + \frac{1}{2}g(h^2 - H^2) \\ hcv_y \end{array} \right\} \tag{3}$$

and being the so-called diffusive flux terms

$$\mathbf{R}_x^{\mathrm{D}} = \left\{ \begin{array}{c} 0 \\ 2h\mu\rho^{-1}\dfrac{\partial}{\partial x}v_x \\ h\mu\rho^{-1}\left(\dfrac{\partial}{\partial x}v_y + \dfrac{\partial}{\partial y}v_x\right) \\ h\gamma\dfrac{\partial}{\partial x}c \end{array} \right\}, \quad \mathbf{R}_y^{\mathrm{D}} = \left\{ \begin{array}{c} 0 \\ h\mu\rho^{-1}\left(\dfrac{\partial}{\partial x}v_y + \dfrac{\partial}{\partial y}v_x\right) \\ 2h\mu\rho^{-1}\dfrac{\partial}{\partial y}v_y \\ h\gamma\dfrac{\partial}{\partial y}c \end{array} \right\} \tag{4}$$

In the above expressions, f is the Coriolis' coefficient, g is the gravity acceleration, H is the average depth at each point (bathymetry), $\boldsymbol{\tau} = [\tau_x, \tau_y]^{\mathrm{T}}$ is the tangential stress due to the wind friction, ρ is the water density, n is the Manning coefficient (modelling the energy losses due to the seabed friction), μ is the dynamic viscosity and γ is the total diffusivity (that includes the combined effect of the molecular diffusion, the turbulent diffusion and the dispersive diffusion [6, 7]).

The Coriolis' coefficient f is defined in terms of the latitude of the place ϕ and of the angular velocity of rotation of the Earth Ω as

$$f = 2\Omega \sin(\phi) \tag{5}$$

Furthermore, the tangential stress due to the wind $\boldsymbol{\tau}$ can be expressed as a quadratic function of the wind velocity $\mathbf{v}_{\mathrm{w}}$ [4] by means of the well-known Ekman's formula:

$$\boldsymbol{\tau} = \kappa|\mathbf{v}_{\mathrm{w}}|\mathbf{v}_{\mathrm{w}} \quad \text{with } \kappa = 3.2 \times 10^{-3}\,\mathrm{Ns^2/m^4} \tag{6}$$

and the total diffusivity γ can be obtained from the depth h and the velocity $\mathbf{v}$ by means of the so-called Elder's formula [6, 7]:

$$\gamma = 0.6h|\mathbf{v}| \tag{7}$$

With regard to the boundary conditions, we have three different situations.

In the part of the boundary that corresponds to the mouth of the Ulla River we can suppose that the flow is super-critical (what precludes the conditions in the estuary to influence the upstream flow). Thus, we prescribe the flux and the salinity as

$$h\mathbf{v}^{\mathrm{T}}\mathbf{n} = -h\frac{Q_{\mathrm{R}}}{A(h)} \quad \text{and} \quad c = 0 \quad \text{on the river} \tag{8}$$

where Q_R is the known volume of flow in the river, $A(h)$ is the area of the wet section of the river and $\mathbf{n}$ is the external normal to the boundary. The salinity c is prescribed to be null, since the river flows fresh water into the estuary.

In the part of the boundary that corresponds to the sea we can suppose that the flow is sub-critical. Thus, we prescribe the depth and the salinity as

$$z = z_S(t) + \Delta z_S \quad \text{and} \quad c = c_S \text{ on the sea} \tag{9}$$

where $z_S(t)$ is the prescribed depth due to the tide harmonics and Δz_S is the so-called meteorological tide. The meteorological tide is the rise or the fall of the surface level during a storm (due to the wind that blows on the whole fetch). It can be obtained from the corresponding measures and records of the seaports authorities.

Finally, we can state that both the flux of water and the flux of salt are null in the direction $\mathbf{n}$ of the normal to the shore, which gives

$$h\mathbf{v}^T\mathbf{n} = 0 \quad \text{and} \quad h\,\mathbf{grad}^T(c)\mathbf{n} = 0 \text{ on the shore} \tag{10}$$

3. NUMERICAL MODEL

The above-stated problem must be solved numerically. In order to do so, we will use the finite element method. More specifically, we will solve the problem by means of a second-order Taylor–Galerkin (TG-2) approach [3, 5, 9, 10].

3.1. Derivation of the TG-2 formulation

In order to derive the Taylor–Galerkin formulation, we first write a Taylor's expansion in the time coordinate of the unknown $\mathbf{u}$:

$$\mathbf{u}|_{t=t_{n+1}} = \mathbf{u}|_{t=t_n} + \frac{\Delta t}{1!} \left.\frac{\partial \mathbf{u}}{\partial t}\right|_{t=t_n} + \frac{\Delta t^2}{2!} \left.\frac{\partial^2 \mathbf{u}}{\partial t^2}\right|_{t=t_n} + \mathcal{O}(\Delta t^3)$$

$$= \mathbf{u}|_{t=t_n} + \Delta t \left[\frac{\partial \mathbf{u}}{\partial t} + \frac{\Delta t}{2}\frac{\partial^2 \mathbf{u}}{\partial t^2}\right]_{t=t_n} + \mathcal{O}(\Delta t^3) \tag{11}$$

Then, we can rewrite the above expansion as

$$\mathbf{u}|_{t=t_{n+1}} = \mathbf{u}|_{t=t_n} + \Delta t \; \mathbf{w}|_{t=t_n} + \mathcal{O}(\Delta t^3) \tag{12}$$

where

$$\mathbf{w} = \left[\frac{\partial \mathbf{u}}{\partial t} + \frac{\Delta t}{2}\frac{\partial^2 \mathbf{u}}{\partial t^2}\right] \tag{13}$$

By taking into account the differential equation (1) we can write

$$\frac{\partial \mathbf{u}}{\partial t} = \mathbf{R}^S - \left(\frac{\partial \mathbf{F}_x}{\partial x} + \frac{\partial \mathbf{F}_y}{\partial y}\right) + \left(\frac{\partial \mathbf{R}_x^D}{\partial x} + \frac{\partial \mathbf{R}_y^D}{\partial y}\right)$$

$$\frac{\partial^2 \mathbf{u}}{\partial t^2} = \frac{\partial}{\partial t}\,\mathbf{R}^{\mathrm{S}} - \frac{\partial}{\partial t}\left(\frac{\partial \mathbf{F}_x}{\partial x} + \frac{\partial \mathbf{F}_y}{\partial y}\right) + \frac{\partial}{\partial t}\left(\frac{\partial \mathbf{R}_x^{\mathrm{D}}}{\partial x} + \frac{\partial \mathbf{R}_y^{\mathrm{D}}}{\partial y}\right)$$

$$= \dot{\mathbf{R}}^{\mathrm{S}} - \left(\frac{\partial \dot{\mathbf{F}}_x}{\partial x} + \frac{\partial \dot{\mathbf{F}}_y}{\partial y}\right) + \left(\frac{\partial \dot{\mathbf{R}}_x^{\mathrm{D}}}{\partial x} + \frac{\partial \dot{\mathbf{R}}_y^{\mathrm{D}}}{\partial y}\right) \tag{14}$$

Therefore, we can rewrite (13) as

$$\mathbf{w} = \left[\frac{\partial \mathbf{u}}{\partial t} + \frac{\Delta t}{2}\frac{\partial^2 \mathbf{u}}{\partial t^2}\right] = \mathbf{b} - \left(\frac{\partial \mathbf{A}_x}{\partial x} + \frac{\partial \mathbf{A}_y}{\partial y}\right) \tag{15}$$

being

$$\mathbf{b} = \mathbf{R}^{\mathrm{S}} + \frac{\Delta t}{2}\dot{\mathbf{R}}^{\mathrm{S}}$$

$$\mathbf{A}_x = \left(\mathbf{F}_x + \frac{\Delta t}{2}\,\dot{\mathbf{F}}_x\right) - \left(\mathbf{R}_x^{\mathrm{D}} + \frac{\Delta t}{2}\,\dot{\mathbf{R}}_x^{\mathrm{D}}\right) \tag{16}$$

$$\mathbf{A}_y = \left(\mathbf{F}_y + \frac{\Delta t}{2}\,\dot{\mathbf{F}}_y\right) - \left(\mathbf{R}_y^{\mathrm{D}} + \frac{\Delta t}{2}\,\dot{\mathbf{R}}_y^{\mathrm{D}}\right)$$

Applying the weighted residuals method in the spatial coordinates to (15) yields

$$\iint_{(x,y)\in\Omega} \varpi\left(\mathbf{w} - \left[\mathbf{b} - \left(\frac{\partial \mathbf{A}_x}{\partial x} + \frac{\partial \mathbf{A}_y}{\partial y}\right)\right]\right)\mathrm{d}\Omega = 0 \quad \forall \varpi \tag{17}$$

that can be rewritten as

$$\iint_{(x,y)\in\Omega} \varpi\mathbf{w}\,\mathrm{d}\Omega = \iint_{(x,y)\in\Omega} \varpi\mathbf{b}\,\mathrm{d}\Omega$$

$$- \iint_{(x,y)\in\Omega} \varpi\left(\frac{\partial \mathbf{A}_x}{\partial x} + \frac{\partial \mathbf{A}_y}{\partial y}\right)\mathrm{d}\Omega \quad \forall \varpi \tag{18}$$

In the previous expression we can replace

$$\varpi\left(\frac{\partial \mathbf{A}_x}{\partial x} + \frac{\partial \mathbf{A}_y}{\partial y}\right) = \left[\frac{\partial}{\partial x}(\varpi\mathbf{A}_x) + \frac{\partial}{\partial y}(\varpi\mathbf{A}_y)\right] - \left[\frac{\partial \varpi}{\partial x}\mathbf{A}_x + \frac{\partial \varpi}{\partial y}\mathbf{A}_y\right] \tag{19}$$

and we can define

$$\underset{\sim}{\mathbf{A}} = [\mathbf{A}_x\ \ \mathbf{A}_y], \quad \mathrm{grad}^{\mathrm{T}}(\varpi) = \left\{\frac{\partial \varpi}{\partial x}\ \ \frac{\partial \varpi}{\partial y}\right\} \tag{20}$$

Now, we can write

$$\left[\frac{\partial \varpi}{\partial x}\mathbf{A}_x + \frac{\partial \varpi}{\partial y}\mathbf{A}_y\right] = \underset{\sim}{\mathbf{A}}\,\mathrm{grad}(\varpi) \tag{21}$$

and by applying the divergence theorem

$$\iint_{(x,y)\in\Omega}\left[\frac{\partial}{\partial x}\left(\varpi \mathbf{A}_x\right)+\frac{\partial}{\partial y}\left(\varpi \mathbf{A}_y\right)\right]d\Omega=\int_{(x,y)\in\partial\Omega}\varpi\underset{\sim}{\mathbf{A}}\mathbf{n}\,d\partial\Omega \tag{22}$$

we finally obtain the variational form of the problem:

$$\iint_{(x,y)\in\Omega}\varpi\mathbf{w}\,d\Omega=\iint_{(x,y)\in\Omega}\varpi\mathbf{b}\,d\Omega+\iint_{(x,y)\in\Omega}\underset{\sim}{\mathbf{A}}\,\text{grad}(\varpi)\,d\Omega$$

$$-\int_{(x,y)\in\partial\Omega}\varpi\underset{\sim}{\mathbf{A}}\mathbf{n}\,d\partial\Omega\quad\forall\varpi \tag{23}$$

Now, if we discretize the trial functions in the form

$$\mathbf{u}(x,y,t)=\sum_I\mathbf{u}_I(t)\phi_I(x,y)$$

$$\mathbf{w}(x,y,t)=\sum_I\mathbf{w}_I(t)\phi_I(x,y) \tag{24}$$

and the test functions in the form

$$\varpi(x,y,t)=\sum_J\boldsymbol{\beta}_J(t)\varpi_J(x,y) \tag{25}$$

we obtain the discretized variational form

$$\sum_I\left[\iint_{(x,y)\in\Omega}\varpi_J\phi_I\,d\Omega\right]\mathbf{w}_I=\iint_{(x,y)\in\Omega}[\varpi_J\mathbf{b}+\underset{\sim}{\mathbf{A}}\,\text{grad}(\varpi_J)]\,d\Omega$$

$$-\int_{(x,y)\in\partial\Omega}\varpi_J\underset{\sim}{\mathbf{A}}\mathbf{n}\,d\partial\Omega\quad\forall J \tag{26}$$

If we now choose the Galerkin method

$$\varpi_J(x,y)=\phi_J(x,y) \tag{27}$$

we finally get the TG-2 expressions.

3.2. Implementation of the TG-2 algorithm

In essence, at each time step the following linear system of equations is solved (space integration):

$$\sum_I[M_{JI}]\mathbf{w}_I(t_n)=\{\mathbf{f}_J\}|_{t=t_n}\quad\text{with}$$

$$[M_{JI}]=\left[\iint_{(x,y)\in\Omega}\phi_J\phi_I\,d\Omega\right]\quad\text{and} \tag{28}$$

$$\{\mathbf{f}_J\}=\left\{\iint_{(x,y)\in\Omega}[\phi_J\mathbf{b}+\underset{\sim}{\mathbf{A}}\,\text{grad}(\phi_J)]\,d\Omega-\int_{(x,y)\in\partial\Omega}\phi_J\underset{\sim}{\mathbf{A}}\mathbf{n}\,d\partial\Omega\right\}$$

Then, the solution is updated (time integration) by neglecting third-order errors, which gives the second-order accurate expression:

$$\mathbf{u}_I(t_{n+1}) = \mathbf{u}_I(t_n) + \Delta t \mathbf{w}_I(t_n) \tag{29}$$

The coefficients matrix in system (28) is the so-called 'mass matrix'. This linear system can be solved by using a diagonal preconditioned conjugate gradient algorithm without assembling the global matrix. Alternatively, the solution to (28) can be approximated by using the so-called diagonal lumped mass matrix [3]. This has been the procedure that was finally used in this project.

4. DISCRETIZATION AND BATHYMETRY

Although the area of interest (*Los Lombos del Ulla*) is relatively small, we are forced to analyse the whole estuary (see Figure 1) in order to impose the sea boundary conditions far enough from the area of interest, and in order to take into account the influence of the whole estuary in the hydrodynamics.

The estuary was discretized by the Gen4u mesh generator [11–14] in 30 970 isoparametric quadrangular elements of four nodes, which yields 120 424 degrees of freedom (d.o.f.) (30 106 nodes times 4 d.o.f. per node) at each time step (see Figure 4). Approximately half of the total elements (14 979) are placed in *Los Lombos del Ulla* while the rest are spread in the rest of the estuary, which is the most extensive part. Thus, 58 144 d.o.f. (14 536 nodes times 4 d.o.f. per node) are devoted to represent the approximate solution in the area of interest.

The size of the elements gradually grows as we move away from *Los Lombos*. Thus, the length of the quadrilaterals ranges from about 20 m (near the mouth of the Ulla River) to about 200 m
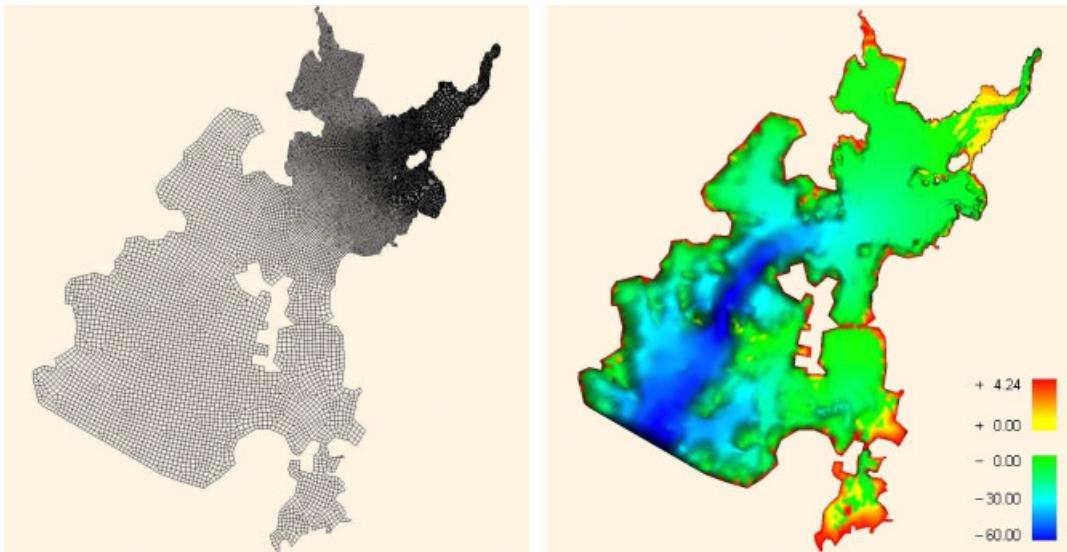

Figure 4. GEN4U discretization of the whole estuary (left). Actual bathymetry (right).

(as we proceed into the Atlantic Ocean). In this way we seek more precise results in the area of interest. But, also, we try to avoid the stability conditions [3] to become excessively restrictive, since the largest elements are located in the deepest areas (where the velocity of propagation of the gravity waves is higher).

In fact, the proposed Taylor–Galerkin formulation performed pretty well (as expected) for quite large time steps (close to the Courant Friedrichs–Lewy limit) that allowed long simulations to be carried out.

The actual bathymetry of the whole estuary was obtained from some measurements specifically made in *Los Lombos* during 2002, from the charts of the estuary and from the available topographic data of the shore [1] (see Figure 4).

The bathymetry that corresponds to the first possible action (dredging a navigation channel) was obtained from the actual bathymetry by dropping the corresponding values of the seabed height down to the level -1.5 m. This action implies the dredging of $614\,651.24\,\text{m}^3$ of solids. The bathymetry that corresponds to the second possible action (general dredging of *Los Lombos*) was obtained from the actual bathymetry by dropping the corresponding values of the seabed height down to the level -0.5 m, but limiting the drop to 0.75 m in each point at the most [1]. This action implies the dredging of $3\,876\,503.49\,\text{m}^3$ of solids.

5. PROGRAM OF SIMULATIONS

Two types of simulations were carried out: 28 days simulations in normal conditions (NC) and 2 days simulations in extreme conditions (EC) [1]. The 28 days simulations compare the results obtained for the actual bathymetry (i.e. the current situation) with the results predicted for each one of the two possible actions (dredging a navigation channel and dredging the whole area of *Los Lombos*). The second option was discarded after analysing these results. Thus, the 2 days simulations only compare the results obtained for the current bathymetry with the results predicted for the first possible action (dredging a navigation channel). In the NC simulations we considered the average volume of water ($Q_R^{\text{MED}} = 56\,\text{m}^3/\text{s}$) in the Ulla River, and the average velocity wind ($\mathbf{v}_W^{\text{MED}} = 4.8\,\text{m/s}$) blowing in the dominant direction (202° S-SW) without meteorological tide ($\Delta z_S = 0$ m). On the other hand, five different ECs were defined: southwest storm (EC#1), flood condition (EC#2), southwest storm and flood condition (EC#3), northeast storm and flood condition (EC#4) and northeast storm (EC#5). In the EC#2, EC#3 and EC#4 simulations we considered the flood volume of water ($Q_R^{\text{MAX}} = 300\,\text{m}^3/\text{s}$) in the Ulla River. In the other ones (EC#1, EC#5) we considered the average volume of water (Q_R^{MED}) in the Ulla River. In the EC#1 and EC#3 simulations we considered the maximum velocity wind ($v_W^{\text{MAX}} = 15.0\,\text{m/s}$) blowing in the most adverse direction (210° SW) with positive meteorological tide ($\Delta z_S = 0.15$ m). In the EC#4 and EC#5 simulations we considered the maximum velocity wind (v_W^{MAX}) blowing in NE direction (30° NE) with negative meteorological tide ($\Delta z_S = -0.15$ m). In the remaining simulation (EC#2) we considered the average velocity wind (v_W^{MED}) blowing in the dominant direction (202° S-SW) without meteorological tide ($\Delta z_S = 0$ m).

We took the following values for the physical constants of the problem: $\Omega = 2\pi/86\,164.09\,\text{rad/s}$, $\phi = 43°\,35'\,58''$, $g = 9.81\,\text{m/s}^2$, $\rho = 10^3\,\text{kg/m}^3$, $n = 0.0425\,\text{s/m}^{1/3}$, $c_S = 0.035$ and $\mu = 50\,\text{kg/ms}$, where the latitude ϕ corresponds to the *Vilagarcía de Arousa* Harbour.

Table I. Main harmonics of the tide (Vilagarcía de Arousa Harbour).

Harmonic	i	A_i (m)	ω_i (rad/s)	φ_i (rad)
Z0	0	2.151	0.000000E+00	0.000000000
M2	1	1.145	0.140518E−03	1.391201947
S2	2	0.401	0.145444E−03	1.920211243
N2	3	0.243	0.137879E−03	1.073377490
K2	4	0.113	0.145841E−03	1.885653724
K1	5	0.077	0.729199E−04	1.140747199
O1	6	0.069	0.675966E−04	5.576676026
L2	7	0.029	0.143157E−03	1.695587368
P1	8	0.025	0.725219E−04	1.004087919
Q1	9	0.021	0.649577E−04	4.809778353
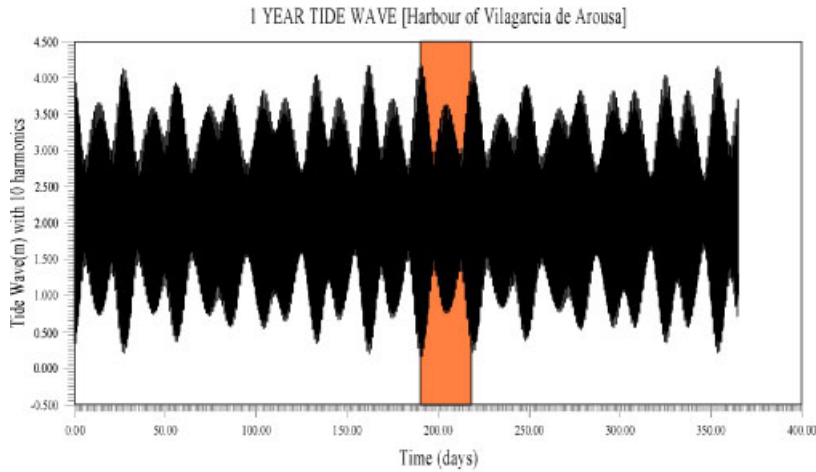
Figure 5. One year tide wave and interval used for the 28 days simulations.

Finally, the tide was modelled by adding up the first 10 harmonics ($n = 9$) of the corresponding Fourier series, as

$$z_S(t) = \sum_{i=0}^{n} A_i \cos(\omega_i t + \varphi_i) \tag{30}$$

where the amplitude (A_i), the angular frequency (ω_i) and the phase (φ_i) of each harmonic (i) have been obtained from the Spanish seaports authority website [15] (see Table I). Figure 5 shows the 1 year tide wave and the 28 days window that was used for the NC simulations. Figure 6 shows the 28 days tide wave and the 2 days window that were used for the NC and for the EC simulations.
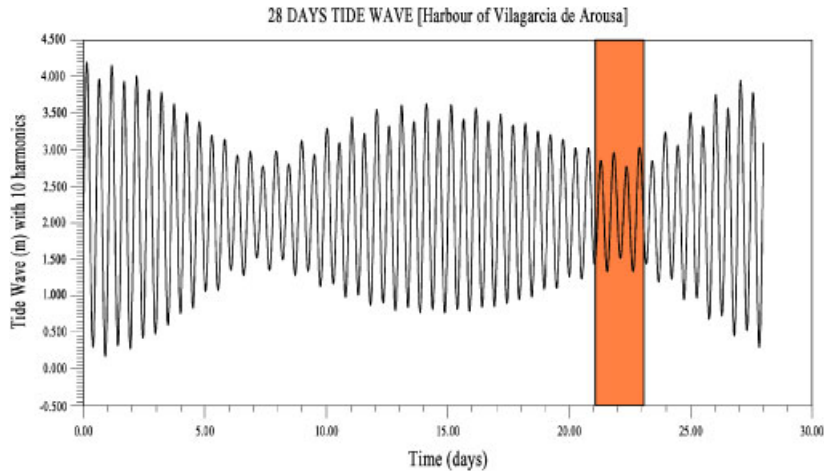
Figure 6. Twenty-eight days tide wave and subinterval used for the 2 days simulations.

6. ANALYSIS OF RESULTS

The numerical results of the model have been compared with the data given by the experts in the hydrodynamics of the area, with measurements performed during the project and with computed results obtained with simpler models. The results agree with the available data and the model predicts correctly the main hydrodynamical phenomena that are observed in the estuary. Some of these features are well documented. Namely, it is well known that the fresh water current progressing downstream tends to get closer to the right shore of the estuary, rather than to the left one. This fact is commonly attributed to the Coriolis' acceleration. Consequently, the salinity in the right shore is lower than in the opposite side. The strong correlation between the salinity level and the fishing productivity becomes apparent when one compares the different density of population and of ancient human settlements on both sides of the estuary. Other facts are not as well known or as easy to explain. Thus, the records of the regional coastal authorities report sudden rises of the salinity level upstream the Ulla River during Northeast storms. Up to what we know, there is not an acceptable physical explanation yet for this feature. Nevertheless, the numerical model is able to reproduce quite accurately all these facts.

The results provided by the numerical model for the actual bathymetry case show that the periodic emptying (almost complete) of *Los Lombos* due to the low tide during the spring tide cycles is the essential process that allows to maintain the average level of salinity in the area (see Figure 7). Thus, the salinity level inexorably falls during the neap tide cycles due to the continuous contribution of fresh water from the river. But it is fully recovered during the spring tide cycles, due to the emptying of most of the basin and to the periodic contribution of salt water from the sea.

Therefore, a general dredging would cause an important decrease in the average salinity level in all the area as it is observed in the corresponding simulations (see Figure 9). For this reason, we absolutely advised against a general dredging of *Los Lombos*. However, the numerical model predicts that the dredging of a navigation channel in the direction of the main stream should not significantly modify the average salinity level in *Los Lombos* (see Figure 8). The results show
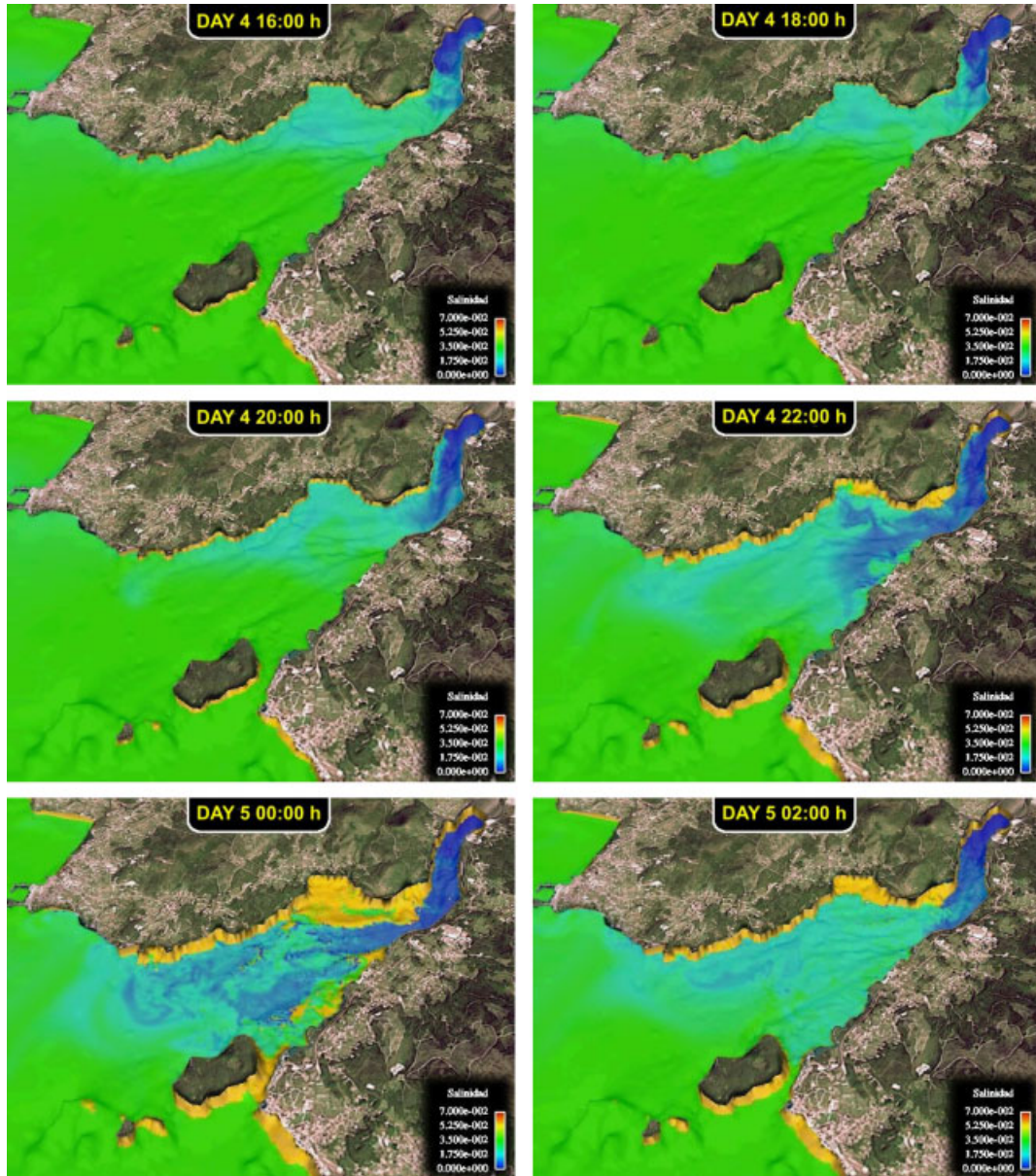
Figure 7. Evolution of the salinity in *Los Lombos* under normal conditions: actual bathymetry case. The salinity level is recovered during the spring tides due to the periodic emptying of the basin and to the subsequent filling with salt water (Intertidal zones in yellow, salt water in green, fresh water in blue).

that the navigation channel would facilitate the emptying and the filling of the basin during the spring tide cycles. Furthermore, the fresh water progressing downstream would be more effectively canalized when the tide is going out, which would contribute to preserve the salinity level in the
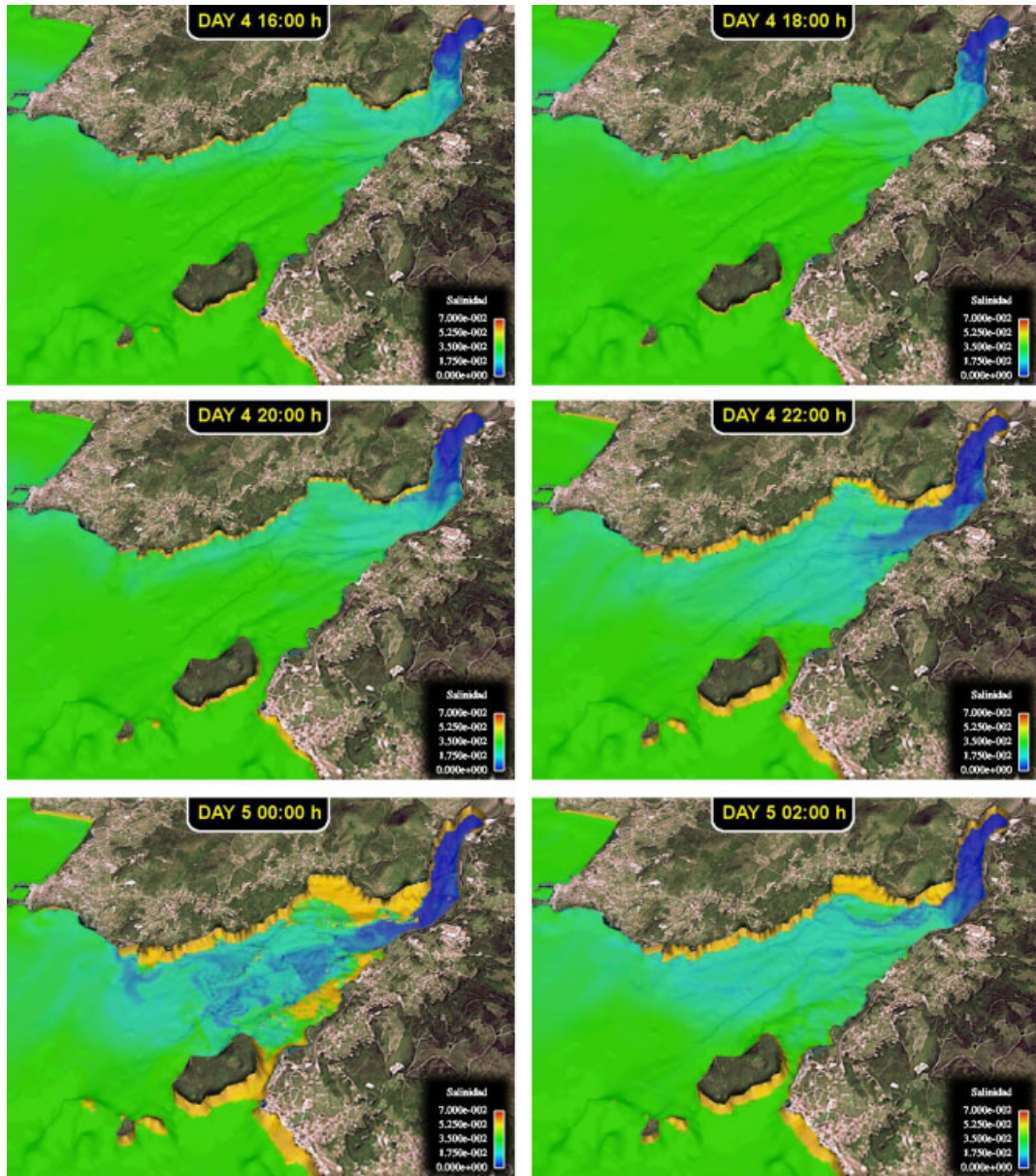
Figure 8. Evolution of the salinity in *Los Lombos* under normal conditions: channel dredging case. The average salinity level would not be significantly modified while the navigation conditions in the area could be improved (Intertidal zones in yellow, salt water in green, fresh water in blue).

rest of the area. Therefore, the average salinity level could slightly raise in these periods. However, the channel would behave like a deeper basin when the tide is very low, which could cause a certain decrease in the average salinity level during the neap tide cycles. When combined, these
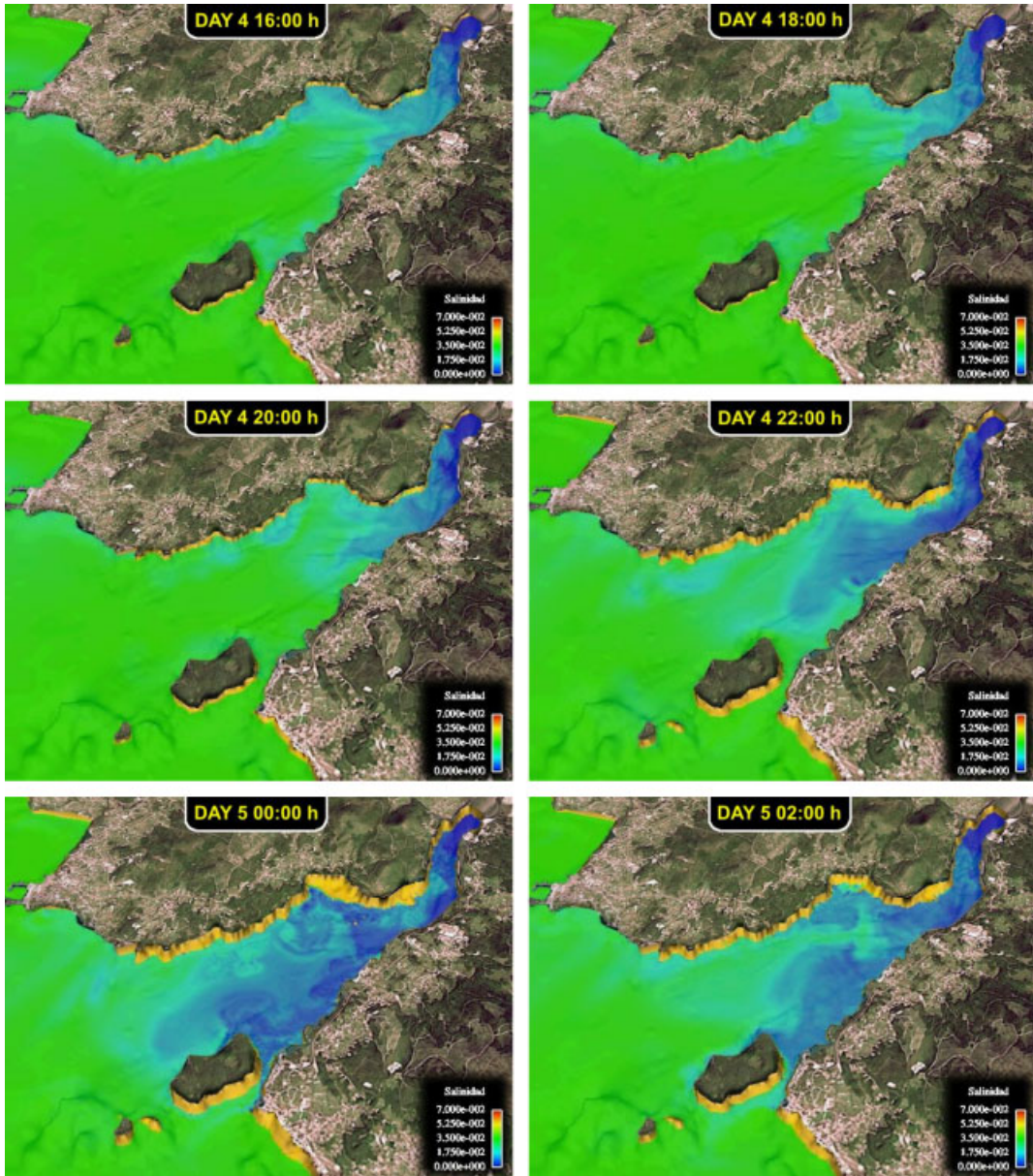
Figure 9. Evolution of the salinity in *Los Lombos* under normal conditions: general dredging case. The salinity level would not be recovered during the spring tide cycles, since the basin would no longer be periodically emptied (Intertidal zones in yellow, salt water in green, fresh water in blue).

opposite effects cancel one to the other. Therefore, the shellfish production of the area would not be substantially affected by the dredging of a channel, while the navigation conditions in the area could be significantly improved.

Due to the above explained results, the general dredging of *Los Lombos* was finally discarded as a valid option. This not only saved the cost of the dredging works themselves (for an estimated amount of several tens of millions of Euros), but it also avoided an unprecedented environmental and economical disaster to occur. On the other hand, the obtained numerical results have been found useful for predicting the migration of the shellfish colonies (depending on the salinity level and on the currents) and for other practical purposes.

7. CONCLUSIONS

In this paper, a numerical model for the simulation of the hydrodynamics and of the evolution of the salinity in shallow water estuaries is presented. The mathematical model considers all the relevant issues, including the effects of the tides (taking into account that the seabed could be exposed), the volume of fresh water provided by the rivers and the effects of the winds. The problem is numerically solved by means of a TG-2 finite element formulation. The presented model provides useful and accurate numerical information that can be used to predict the possible effects of Civil Engineering public works and other human actions (i.e. dredging, building of docks, spillages, etc.) and to evaluate their environmental impact. Furthermore, it contributes to knowing better the marine habitat by showing how important are the different processes involved in the hydrodynamics of an estuary, while the obtained numerical results can be used for other practical purposes (i.e. for predicting the migration of the shellfish colonies depending on the salinity level and on the currents).

REFERENCES

1. Navarrina F. Modelo Numérico de los Lombos del Ulla: Informe Final. *Technical Report*, Fundación de la Ingeniería Civil de Galicia—Universidad de A Coruña, Coruña, 2004.
2. Navarrina F, Colominas I, Casteleiro M, Cueto-Felgueroso L, Gómez H, Fe J, Soage A. Analysis of hydrodynamic and transport phenomena in the Ría de Arousa: a numerical model for high environmental impact estuaries. In *Fluid Structure Interaction and Moving Boundary Problems*, Chakrabarti SK, Hernández S, Brebbia CA (eds). WIT Press: Southampton, 2005; 583–593.
3. Peraire J, Zienkiewicz OC, Morgan K. Shallow water problems: a general explicit formulation. *International Journal for Numerical Methods in Engineering* 1986; **22**:547–574.
4. Scarlatos PD. Estuarine hydraulics. In *Environmental Hydraulics*, Singh VP, Hager WH (eds). Kluwer Academic Publishers: Dordrecht, 1996; 289–348.
5. Peraire J. A finite element method for convection dominated flows. *Ph.D. Thesis*, University College of Swansea, Swansea, 1986.
6. Fischer HB *et al*. *Mixing in Inland and Coastal Waters*. Academic Press Inc.: Orlando, FL, 1979.
7. Holley ER. Diffusion and dispersion. In *Environmental Hydraulics*, Singh VP, Hager WH (eds). Kluwer Academic Publishers: Dordrecht, 1996; 111–151.

Int. J. Numer. Meth. Fluids 2008; **56**:507–523
                                                                       DOI: 10.1002/fld

8. Rutherford JC. *River Mixing*. Wiley: Chichester, 1994.
9. Donea J, Huerta A. *Finite Element Methods for Flow Problems*. Wiley: Chichester, 2003.
10. Zienkiewicz OC, Taylor RL. *The Finite Element Method*, *Vol. III*: *Fluid Dynamics*. Butterworth–Heinemann: Oxford, 2000.
11. Sarrate J. Modelización numérica de la interacción fluido-sólido rígido: desarrollo de algoritmos, generación de mallas y adaptabilidad. *Ph.D. Thesis*, Universitat Politècnica de Catalunya, Catalunya, 1996.
12. Sarrate J, Huerta A. Efficient unstructured quadrilateral mesh generation. *International Journal for Numerical Methods in Engineering* 2000; **49**:1327–1350.
13. Sarrate J, Huerta A. Manual de Gen4u (versión 2.1). *Technical Report*, LaCàN, Universitat Politècnica de Catalunya, Catalunya, 2001.
14. Soage A. Simulación numérica del comportamiento hidrodinámico y de evolución de la salinidad en zonas costeras de gran impacto ambiental: aplicación a la Ría de Arousa. *M.Sc. Thesis*, Escuela Técnica Superior de Ingenieros de Caminos, Canales y Puertos, Universidad de A Coruña, Coruña, 2005.
15. Ente Público Puertos del Estado. *Web de Puertos del Estado* (http://www.puertos.es). Ministerio de Fomento: Madrid, 2004.